Proceedings of ICFDP7:
Seventh International Congress on Fluid Dynamics and Propulsion
December 18-20, 2001, Cairo, Egypt

ICFDP7-2001059

NUMERICAL SIMULATIONS OF TRANSONIC FLOW ACOUSTIC RESONANCE IN CAVITY

A. Hamed, D. Basu, and K. Das
Department of Aerospace Engineering & Engineering Mechanics
University of Cincinnati
Cincinnati, Ohio

ABSTRACT

Direct numerical simulations are used to investigate transonic flow acoustic resonance in an open cavity. The numerical scheme minimizes the errors due to dispersion and dissipation of acoustic waves, and resolves both the unsteady flow and radiated acoustic field. Implicit solution of the compressible Navier-Stokes equations is obtained using a compact high-order spacial differencing scheme, coupled with high-order implicit filters. Second order temporal accuracy is achieved using a time-implicit approximately-factorization, and Newton-like subiterations. Computational results are presented at sequential times to show the vortical structure and shock waves at two transonic free stream Mach numbers. The corresponding acoustic response is presented for the pressure fluctuations and sound pressure level spectra near the rear bulkhead. Comparison of the computed discrete frequencies with Rossiter's correlation indicates that the feedback mechanism, which induces self-sustained flow oscillations in the cavity is well captured.

Introduction

High-speed flow over deep open cavities is characterized by shear layer instability and acoustically dominated flow oscillations. Strong pressure fluctuations inside the cavity, intensive noise radiation, and large shock motion negatively impact the operation and structural integrity. Recent interest in cavity acoustic resonance is motivated by the need to develop flow control strategies to reduce acoustic emissions from aircrafts and insure the structural integrity of weapons bays. Current bay spoilers fail to provide adequate acoustic suppression above Mach one. Some degree of acoustic suppression control has been achieved experimentally by stimulating the shear layer spanning the bay with various actuators [1,2]. Optimizing the performance of these devices requires detailed knowledge of the unsteady flow field.

Many numerical investigations of high-speed flow over open cavities [3] are based on the solution of the time dependent Reynolds-Averaged Navier-Stokes equations [4,5]. Colonius et al. [6], used Direct Numerical Simulations (DNS) to study unsteady subsonic flow over two-dimensional cavities, and predicted transition from the shear layer mode to the wake for higher Mach numbers and cavity length to depth ratios. Shieh and Morris [7] used Detached Eddy Simulations (DES) to study subsonic cavity flow, and predicted the wake mode in the two-dimensional but not in the three-dimensional results. They reported better agreement with Rossiter's correlation [8] for the three-dimensional results. Henderson et al. [9] presented computational and experimental results for the Sound Pressure Level (SPL) at the cavity floor.

Direct numerical simulations are used in the current investigation to study transonic flow over two-dimensional cavities. The results obtained using high order compact differencing in conjunction with high order non-dispersive filters, are presented for the vorticity and Mach number contours to illustrate the roll up vortex structure in the shear layer and the shock waves motion at two transonic free stream Mach numbers. Sample pressure fluctuations, and sound pressure level spectra are presented at the cavity opening near the rear bulkhead. The computed results are

compared with Rossiter's modified correlation for discrete frequencies.

Methodology

Direct numerical solutions were obtained for the full compressible Navier-Stokes equations using FDL2DI, whose features are summarized in Table 1. In the present investigation a sixth-order compact formula (C45654). was used in the interior points, with fifth and fourth orders near the boundary [10]. The implicit filtering scheme ($F10^{0.3}$- 0.2.4.6.8.10) is tenth order in the interior [11], with a free parameter $\alpha_f = 0.3$. The equations were normalized using the cavity depth, free stream velocity, and free stream density. The unsteady solution was advanced using implicit time marching with a non-dimensional time step of 2.0×10^{-3}.

The computational domain for the cavity with a length to depth ratio of two (L/D=2), allowed the laminar boundary layer to develop on the flat plate, which extended 4.95D upstream of the cavity's forward bulkhead. Characteristic conditions were applied for subsonic free stream, and first order extrapolation was applied for supersonic free stream at the upper boundary, which was at 9.35D above the cavity opening. First order extrapolation was applied at the downstream boundary, 10.41D behind the rear bulkhead. The computational grid included 143x129 points inside the cavity, and 330x95 points on and above the plane of cavity opening. The grid was clustered with a minimum spacing of 1.0×10^{-4} D.

Results and Discussions

Results are presented for a Reynold's number of 3,000 based on the cavity length. The momentum thicken, θ, of the incoming laminar boundary layer corresponded to $L/\theta = 52.8$. Sample vorticity and Mach number contours from the direct numerical simulations are presented for two transonic free-stream Mach numbers of 0.9 and 1.1 in Figures 1 through 4. The roll up vortical structures in the shear layer and the counter rotating vorticity (opposing sign to the incoming boundary layer) near the cavity walls and floor can be seen in Figures 1 and 2. Comparing the two Figures one can notice the increase in vortex size with free stream Mach number. However large scale shedding reported by Colonius [6] for subsonic flow in the wake mode was not observed. The Mach number contours of figures 3 and 4 show increased shock strength with Mach number.

The pressure fluctuations at the cavity opening, close to the rear bulkhead, are presented in figure 5. One can see that the pressure fluctuations amplitude doubles as the free-stream Mach number increases from Mach 0.9 to 1.1. Figure 6 presents the, SPL spectra, calculated from the pressure fluctuations using 65536 sample points. The discrete frequencies determined from the spectra are presented in Figure 7, and compared to Rossiter's modified empirical correlation for feedback frequencies [12] based on the coupling of the acoustic and vorticity fields:

$$St_m = \frac{f_m L}{U_\infty} = \frac{m - \alpha}{M_\infty / \sqrt{1 + \frac{\gamma - 1}{2} M_\infty^2} + \frac{1}{k}}$$

where St_m is the Strouhal number, U_∞, and M_∞ are free stream velocity and Mach number, f_m is the resonant frequency corresponding to the m mode. The constants α, and k were determined experimentally to be 0.25, and 0.57 by Heller et al. [12], for cavities with L/D greater than four. According to Figure 7, the computed frequencies agree within 6% with Rossiter's equation for the first mode, m=1.

The effect of free-stream Mach number on the computed SPL at the cavity opening is presented in Figure 8, including computed subsonic flow results [13]. Henderson et al. [9] presented experimental data for SPL at the cavity floor at Mach 0.85, 0.98, and 1.19 that exhibited similar trends, but the levels were higher for their L/D=5 cavity.

Conclusions

The presented results for the unsteady two-dimensional flow over a rectangular cavity demonstrate that the direct numerical simulations captured the flow main features including the vortex shedding, shock waves and coupling of the acoustic and vorticity fields. Future plans include Large Eddy simulations of acoustic suppression through high frequency forcing of turbulent supersonic flow over L/D = 4 cavity.

Acknowledgement

This work was supported by DAGSI, Project Number VA-UC-00-01, Dr. Frank Moore Grant monitor.

References

1. Stanek, M. J., Raman, G., Kibens, V., Ross, J. A., Odedra, J., Peto, J.W., 2000, "Control of Cavity Resonance Through Very High Frequency Forcing," AIAA 2000-1905.
2. Stanek, M. J., Raman, G., Kibens, V., Ross, J. A., Odedra, J., Peto, J.W., 2001, "Suppression of Cavity Resonance Using High

Frequency Forcing – The Characteristic Signature of Effective Devices," AIAA 2001-2128.
3. Grace, S., 2001, "An Overview of Computational Aeroacoustic Techniques Applied to Cavity Noise Prediction," AIAA 2001-0510.
4. Shih, S.H., Hamed, A. and Yeuan, J.J., 1994, "Unsteady Supersonic Cavity Flow Simulations Using Coupled k-ε and Navier-Stokes Equations," AIAA Journal, Vol. 32, No. 10, pp 2015-2021.
5. Rizzetta, D. P., 1988, "Numerical Simulations of Supersonic Flow Over a Three-Dimensional Cavity," AIAA Journal, Vol. 26, No. 7, pp 700-807.
6. Colonius, T., Basu, A. J., and Rowley, C. W., 1999, "Numerical Investigation of the Flow Past a Cavity," AIAA 99-1912.
7. Shieh, C. M., and Morris, Philip, J., 2001, "Comparison of two- and three-dimensional turbulent Cavity Flows," AIAA-2001-0511.
8. Rossitter, J.E., 1964, "Wind-Tunnel Experiments on the Flow over Rectangular Cavities at Subsonic and Transonic Speeds," Royal Aircraft Establishment Reports and Memoranda, No. 3438.
9. Henderson, J., Badcock, K. J., and Richards, B. E., 2000, "Understanding Subsonic and Transonic Open Cavity Flows and Suppression of Cavity Tones," AIAA 2000-0658.
10. Gaitonde, D., and Visbal, M. R., 1999, "Further Development of a Navier-Stokes Solution Procedures Based on High-Order Formulas," AIAA 1999-0557.
11. Gaitonde, D., and Visbal, M. R., 2000, "Pade-Type Higher-Order Filters for the Navier-Stokes Equations," AIAA Journal, Vol. 38, No. 11, pp 2103-2112.
12. Heller, H. H., Holmes, G., and Covert, E., 1970, "Flow-Induced Pressure Oscillations in Shallow Cavities," AFFDRL-TR-70-104.
13. Hamed, A., Basu, D., Mohamed, A. and Das, K., 2001, "Direct Numerical Simulations of Unsteady Flow over Cavity," Proceedings 3rd AFOSR International Conference on DNS/LES (TAICDL), Arlington, Texas.

Table 1. Features of FDL2DI Code

Numerics	• Finite difference discretization of compressible NS equations in strong conservation form and general curvilinear co-ordinates. • Pade-Type tri-diagonal based sixth and fourth order compact difference formulation. • Provisions for 3rd order MUSCL based upwind biased Roe scheme and standard 2nd order central differencing. • Implicit filtering up to 10th order, based on the Pade type formulation • Explicit low-storage form of the Runge-Kutta (RK4) method for time integration wave propagation problems. • Implicit second order accurate approximately factored diagonalised Beam and Warming method with Newton-like subiterations for time integration of wall-bounded flows with highly clustered meshes. • Multidomain decomposition with overset mesh capability
Turbulence	• Baldwin-Lomax model • k-ε formulation with compressibility/ vortical upgrades and low Re near wall formulations • LES Subgrid Scale Models
Validations	• Subsonic boundary layers • Wave propagation of acoustic sources • Direct Numerical Simulation of Forced Transitional jet • Flow past a pitching airfoil using moving and deforming meshes • Large Eddy Simulation of supersonic flow over compression ramp

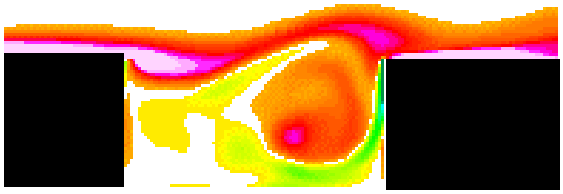

T=100

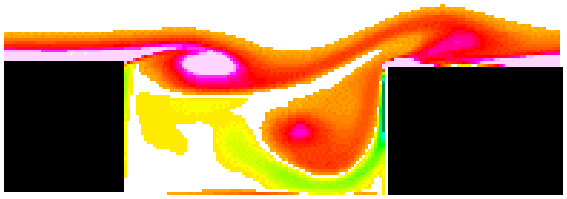

T=102

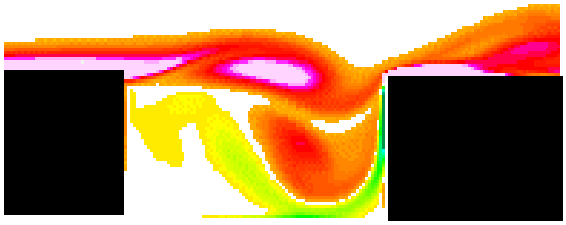

T=104

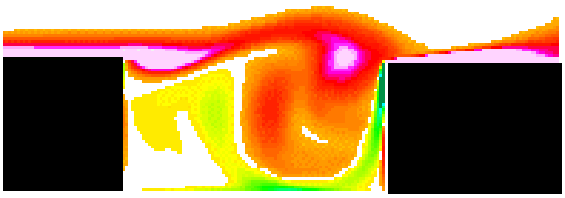

T=106

Fig. 1 Vorticity contours for M_∞ = 0.9

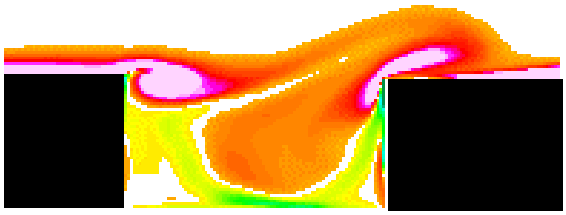

T=100

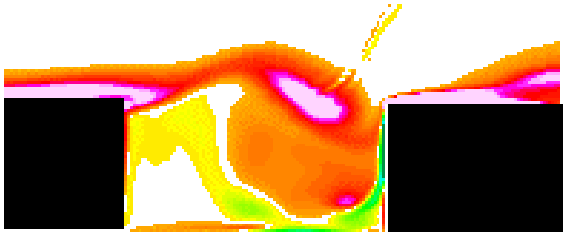

T=102

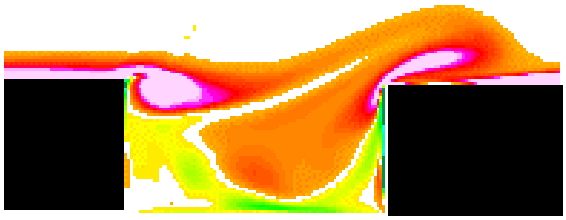

T=104

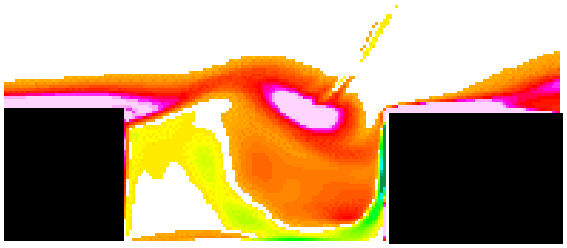

T=106

Fig. 2 Vorticity contours for M_∞ = 1.1

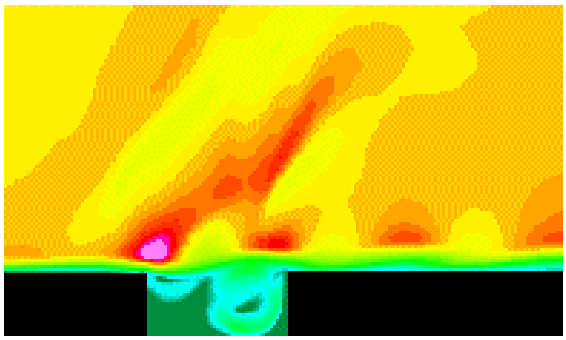

T=100

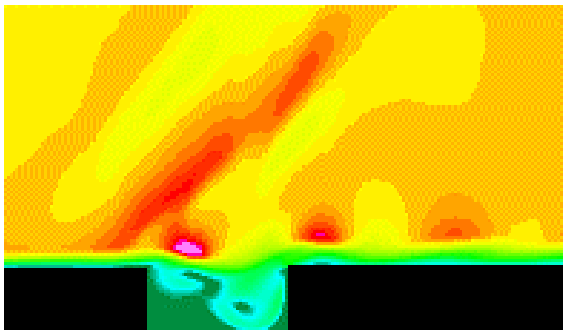

T=102

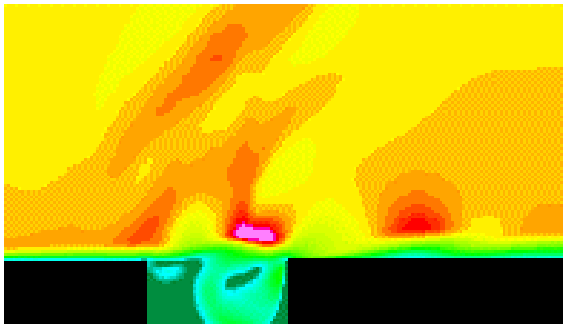

T=104

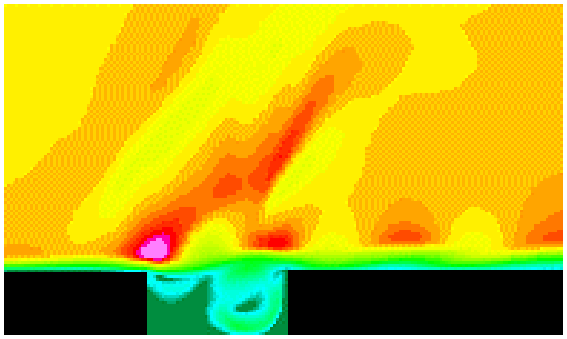

T=106

Fig. 3 Mach number contours for M_∞ = 0.9

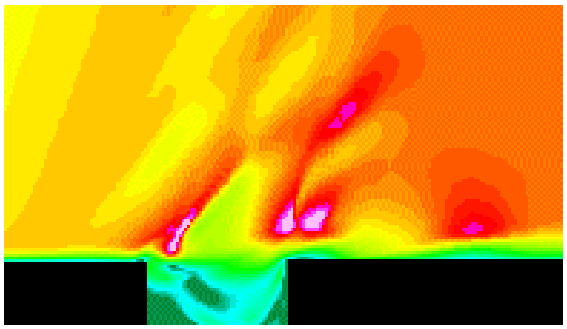

T=100

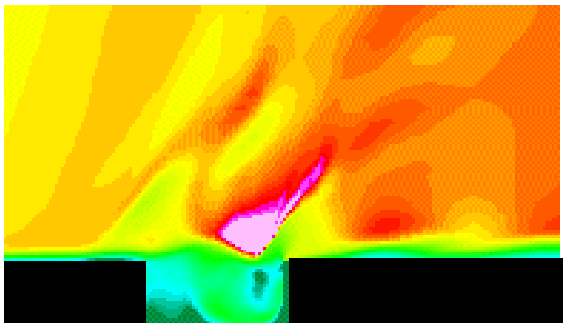

T=102

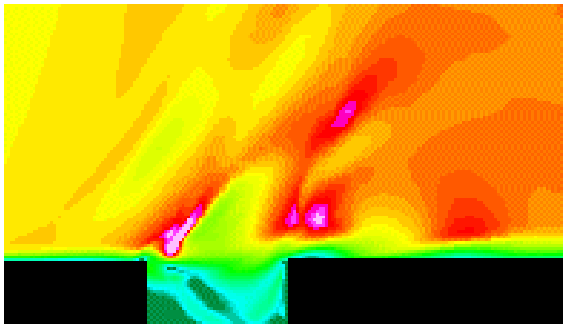

T=104

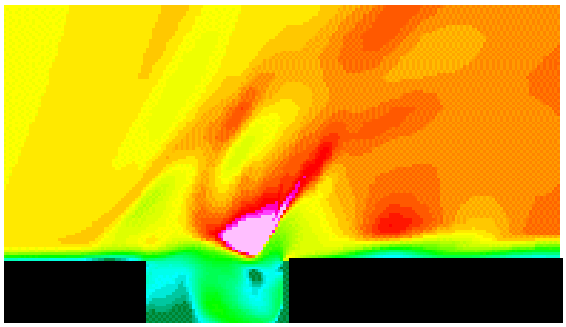

T=106

Fig. 4 Mach number contours for M_∞ = 1.1

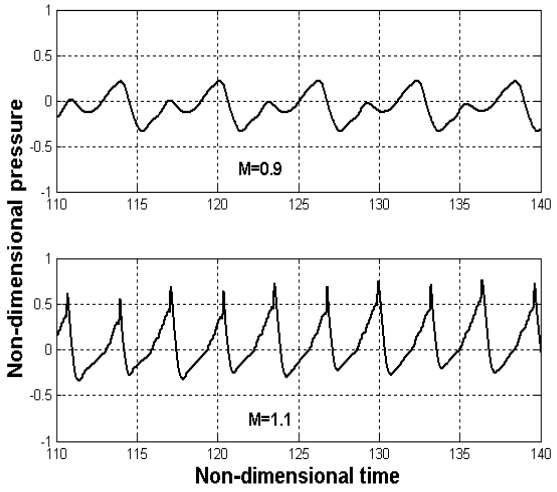

Fig. 5 Perturbation pressure history at cavity opening

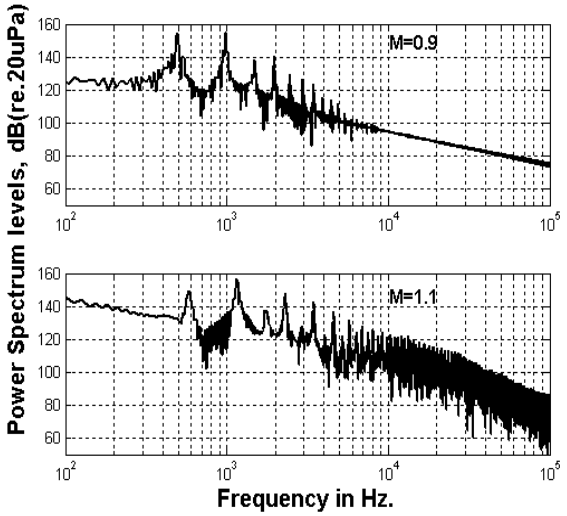

Fig. 6 Sound Pressure level (SPL)

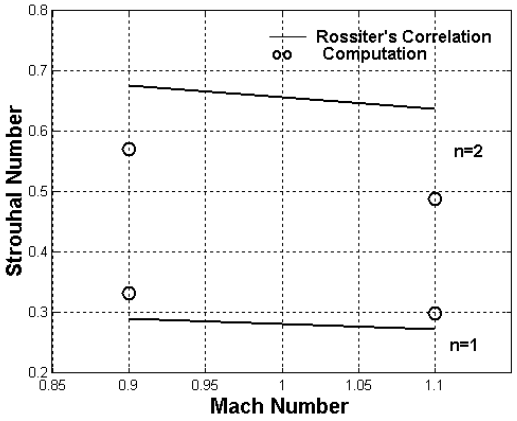

Fig. 7 Comparison of computed discrete frequencies with Rossiter's correlation

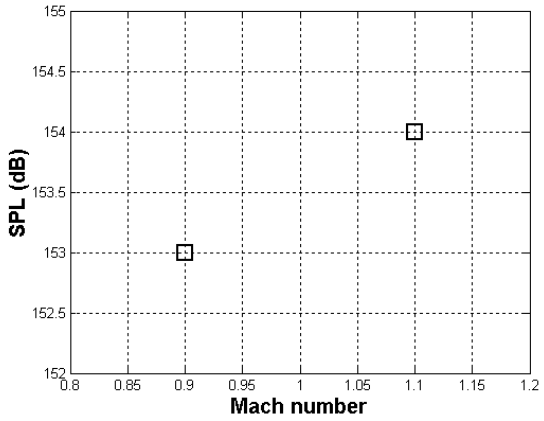

Fig. 8 Variation of sound pressure level with Mach number